VTT Technical Research Centre of Finland

Cannabis detection with solid sensors and paper-based immunoassays by conjugating antibodies to nanocellulose

Solin, Katariina; Vuoriluoto, Maija; Khakalo, Alexey; Tammelin, Tekla

Published in:
Carbohydrate Polymers

DOI:
10.1016/j.carbpol.2022.120517

Published: 15/03/2023

Document Version
Publisher's final version

Carbohydrate Polymers 304 (2023) 120517

Contents lists available at ScienceDirect

Carbohydrate Polymers

journal homepage: www.elsevier.com/locate/carbpol

Cannabis detection with solid sensors and paper-based immunoassays by conjugating antibodies to nanocellulose

Katariina Solin [1], Maija Vuoriluoto [1], Alexey Khakalo [*], Tekla Tammelin [*]

VTT Technical Research Centre of Finland Ltd., Tietotie 4E, FI-02044 Espoo, Finland

ARTICLE INFO

Keywords:
THC detection
Antibody immobilization
Immunoassays
Surface plasmon resonance
Paper-based diagnostics

ABSTRACT

Highly sensitive and specific diagnostics for cannabis usage are essential for rapid on-site screening for illicit drug usage. To improve the sensitivity of THC immunoassays, a proper immobilization of the sensing elements on the sensor substrate is critical. In this work, we demonstrated the utilization of EDC/NHS coupling chemistry with nanocellulose to obtain efficient anchor layers for the immobilization of anti-immune complex antibodies on surfaces. In our approach, the high surface-to-volume ratio, OH-group-rich surface, and high hygroscopicity of TOCNF enable efficient surface functionalization and enhance water permeation inside the nanocellulose network structure, offering a hydrophilic spacer for the sensing antibodies. THC detection was shown in both SPR (surface plasmon resonance technique) and paper-based sensing systems. In SPR, antibody immobilization and the related interactions with the target molecule complex with 1–10 μg/mL THC were followed in-situ in aqueous environment, revealing robust attachment of the antibody to the nanocellulose layer and preserved bioactivity. Additionally, quantitative THC detection was enabled on paper substrate by colorimetric means by employing labeled anti-THC Fab antibody fragments as detection antibodies. THC detection efficiency of covalently linked biointerface was superior compared to the performance of physically linked biointerface. The chemical conjugation of anti-IC to nanocellulose allowed efficient binding, whereas supramolecular conjugation led to insufficient binding, highlighting the relevance of the developed nanocellulose-based anchor layer.

1. Introduction

Cannabis or marijuana is a plant with psychoactive effects used for drug, recreational, and medicinal purposes. It is the most used illicit drug worldwide according to UN World Drug Report 2021 with approx. 200 million users (United Nations Office on Drugs and Crime, 2021). The main psychoactive constituent of cannabis is (−)-Δ^9-Tetrahydrocannabinol (THC), which binds to the cannabinoid receptors in the central nervous system and causes a high sensation or sense of euphoria (Niemi et al., 2010; Zuurman et al., 2009). THC and its derivates are used as target molecules to reveal the usage of cannabis. For instance, THC-based testing is performed during medical screening, workplace drug screening, or to detect possible influence in accidents or crimes such as DUID (driving under influence of drugs).

In the human body, THC is broken down by the liver into several inactive metabolites, such as 11-nor-9-carboxy-Δ^9-tetrahydrocannabinol (THC-COOH), which are the most common target molecules in drug testing for cannabis (Helander et al., 2021; Huestis et al., 1996). These metabolites are usually analyzed from urine or blood in laboratory facilities. The active THC compound can also be detected with blood and saliva-based tests (Berthet et al., 2016; Kidwell et al., 1998). Especially, saliva-based tests are gaining interest due to the increased need for point-of-care (POC) testing. POC tests are low-cost, portable devices, which allow collection and analysis of the sample at the same place, enabling faster testing without the need for medical personnel. These tests are, however, usually presumptive and may need a confirmatory test to verify a positive result (Kale, 2019). Reported THC saliva tests include e.g., colorimetric and fluorescence-based lateral flow assays (LFAs) (Plouffe & Murthy, 2017; Thapa et al., 2020), electrochemical affinity-based biosensors (Stevenson et al., 2019), competitive volumetric-bar-chart chip assays (Li et al., 2017), giant magnetoresistive-based biosensors (Lee et al., 2016), and dye-displacement assays based on utilization of aptamers (Alkhamis et al., 2021). The developed sensors are often based on immunosensing, where the presence of the target molecules in a sample is measured by utilizing highly specific antibodies. To develop highly accurate, sensitive assays,

* Corresponding authors.
E-mail address: alexey.khakalo@vtt.fi (A. Khakalo).
[1] These authors contributed equally.

https://doi.org/10.1016/j.carbpol.2022.120517
Received 4 October 2022; Received in revised form 19 December 2022; Accepted 28 December 2022
Available online 30 December 2022

the antibodies or other sensing elements need to be immobilized properly on the assay supports. Poor attachment can cause loss of bioactivity or lead to detachment of the sensing elements with the applied sample fluids. Moreover, possible low concentrations of THC in samples, which is typical in saliva samples after hours from consumption, are challenging to detect with insufficiently bound antibodies (Niemi et al., 2010).

Typically, nitrocellulose is used in LFAs as rection membrane since it can bind proteins irreversibly and enables a good signal-to-noise ratio upon sensing reactions (Yetisen et al., 2013a). Nevertheless, nitrocellulose has disadvantages such as high flammability, short shelf-life, and low mechanical strength (O'Farrell, 2009; Yetisen et al., 2013b). In addition, commercial nitrocellulose flow membranes are often hydrophobic, therefore, surfactants are usually required to obtain desired flow properties for LFAs. The surfactant can then cause incompatibility issues with sensing reagents and limit protein binding on the sensing areas (Yetisen et al., 2013a). For sensing reagent immobilization, carbodiimide crosslinker chemistry is a well-known immobilization method for the conjugation of antibodies on surfaces. Specifically, materials consisting of carboxyl and/or amine groups facilitate the utilization of N-(3-Dimethylaminopropyl)-N′-ethylcarbodiimide hydrochloride (EDC) and N-hydroxysuccinimide (NHS) chemistries to covalently link proteins onto these materials. For example, cellulose-based materials like TEMPO-oxidized cellulose nanofibrils (TOCNF) and carboxymethyl cellulose (CMC) consist of carboxyl groups on their surface, making them suitable for the preparation of cellulose-based bioactive surfaces (Arola et al., 2012; Lam et al., 2017; Mahmoudifard et al., 2016; Orelma et al., 2014; Orelma, Filpponen, et al., 2012; Orelma, Johansson, et al., 2012; Orelma, Teerinen, et al., 2012; Raghav & Srivastava, 2016; Stanković et al., 2020; Vuoriluoto et al., 2017). Among others, human immunoglobulin G (hIgG) antibodies have been conjugated with EDC/NHS chemistry onto TOCNF films, creating bioactivity (Orelma, Johansson, et al., 2012). Indeed, cellulose filters and chromatography paper as well as nanocellulose materials have been proposed as substrates for diagnostics (Arola et al., 2012; Orelma, Johansson, et al., 2012; Orelma, Teerinen, et al., 2012; Pelton, 2009; Ratajczak et al., 2022; Solin et al., 2020, 2019). Cellulose is an interesting material for diagnostics since it offers a sustainable platform for sensing with many desired qualities such as high availability, biocompatibility, low cost and toxicity. Besides, inherent hygroscopicity and hydrophilicity of cellulose facilitates water interactions and is advantageous for water-based analytics and thus allows various materials design for biosensing applications in aqueous environment (Hakalahti et al., 2017; Heise et al., 2021). However, despite the accomplished advances in nanocellulose-based sensing platforms by the cited studies, drug detection based on the use of TOCNF as an anchor layer for sensing elements is still an area that has not been explored.

In this work, we developed a facile way to produce a selective cannabis detection template by using a nanocellulose-based anchoring substrate coupled with EDC/NHS conjugation strategy. We immobilize sensing reagents on assay supports, both solid ultrathin films and cellulose fiber-based substrates to obtain proof-of-concept detection for THC. The THC detection involving the immobilization procedure was followed using surface plasmon resonance (SPR) and finally demonstrated with the paper-based sensing system. Here, TOCNF layers either on SPR sensors or on the test and control areas of paper-based assays were activated with EDC/NHS chemistry to conjugate THC immune complex specific capture antibodies (anti-IC Fab) on these surfaces. Specifically, both THC antibody fragment (anti-THC Fab) and THC needed to be present to obtain binding onto the prepared biointerface. Scheme 1 shows a schematic illustration of antibody conjugation on TOCNF with EDC/NHS chemistry and subsequent binding of the target immune complex on the immobilized anti-IC. SPR-based detection system enabled the study of antibody immobilization and the related water-based interactions with the target molecule complex in-situ. In addition, the THC detection performance of the biointerface with conjugated antibodies was compared to physically adsorbed antibodies. The effect of surface charge on supramolecular interactions was investigated by comparing anti-IC adsorption on TOCNF (high negative charge) and regenerated cellulose (neutral charge) surfaces. The development of an aqueous detection system is hypothesized to be advantageous since water molecules affect interactions that determine protein-ligand binding affinity and hydrogen bonding is central to biological processes (Ladbury, 1996; Schiebel et al., 2018). Additionally, the swelling of nanocellulose in water offers a hydrophilic spacer for sensing elements, which has been found advantageous for retaining the functional activity of immobilized biological macromolecules (Shmanai et al., 2001). Plant-sourced cellulosic (nano)materials possess superior features as green and sustainable membranes and sensor elements due to their inherent film-forming tendency and large surface area rich in OH-groups. These features offer high hygroscopicity, antifouling tendency, and numerous sites for surface functionalization (Aguilar-Sanchez, Jalvo, Mautner, Nameer, et al., 2021; Aguilar-Sanchez, Jalvo, Mautner, Rissanen, et al., 2021; Heise et al., 2021). Exceptionally beneficial for our approach is the high surface-to-volume ratio of TOCNF coupled with high hygroscopicity; many adsorption sites are available for enrichment and removal of specified compounds whereas high hygroscopicity enhances the water and analyte permeation inside the network structure as evidenced in nanoplastic capturing (Leppänen et al., 2022). In order to effectively utilize short-range interactions for detection, the analyte must be attracted to the close vicinity of the sensor surface, which is the precise task of the nanocellulosic network enabled by its high hygroscopicity. Moreover, colorimetric paper-based assays were developed for THC detection on filter paper. In these assays, the sensing areas were formed by pipetting TOCNF on test and control zones, followed by activation and antibody immobilization. Colorimetric responses were

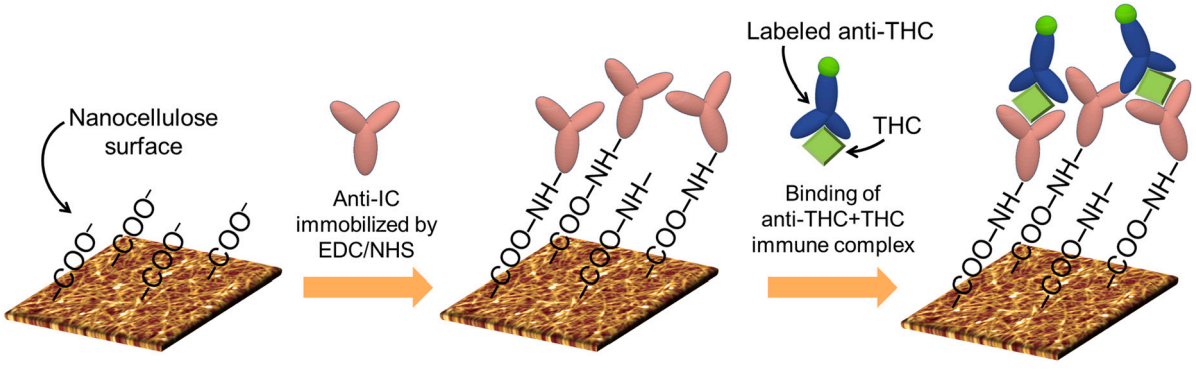

Scheme 1. Schematic illustration of THC detection system based on immobilization of sensing elements on nanocellulose. The specific THC anti-immune complex (anti-IC) antibody is immobilized by EDC/NHS coupling via the formation of an amide bond between the carboxyl groups of TOCNF and the primary amine groups of the antibodies. The formed biointerface enables the binding of the anti-THC + THC immune complex.

obtained by monitoring the binding of horseradish peroxidase (HRP)-labeled target molecule complex (anti-THC + THC) to the immobilized capture antibody on the paper assays. We hypothesize that with this approach, we can easily control robust deposition of sensing elements on the desired sites on a substrate, reducing the risk of antibody removal upon flowing of sample liquids. In addition, nanocellulose anchor enables also scaling-up since its suitability with existing paper-processing technologies such as gravure and inkjet printing, offering more precise deposition and possibility for patterning of large areas. Moreover, our approach that relies on the high anionic charge density of oxidized cellulose nanofibrils offers numerous options for functionalization to obtain selective immobilization of antibodies, and furthermore, enables the utilization of multiple detection methods varying from solid sensor substrates to POC paper-based assays.

2. Experimental

2.1. Materials

(2,2,6,6-Tetramethyl-piperidin-1-yl)oxyl (TEMPO #426369), N-hydroxysuccinimide (NHS #130672), 1-ethyl-3-[3-dimethylaminopropyl]cardodiimide hydrochloride (EDC #03450), bovine serum albumin (BSA), anti-mouse IgG (Fab specific) antibody produced in goat (#M4155), Δ^9-Tetrahydrocannabinol solution (THC #T2386), ethanolamine (#02400), and Whatman® Grade 4 filter paper were acquired from Sigma-Aldrich (Helsinki, Finland). Premium grade EDC (#PG82079) and 1-Step™ ABTS Substrate Solution (#37615) were purchased from Fisher Scientific (Vantaa, Finland). All used laboratory chemicals were of analytical grade. Deionized water further purified with a Millipore Synergy UV unit (Milli-Q) was used in all experiments. The amino acid sequences of the used antibody fragments (anti-IC Fab and anti-THC Fab) are reported in a patent filed by VTT (Takkinen et al., 2011).

In this work, THC detection was investigated on TEMPO-oxidized cellulose nanofibril (TOCNF) and regenerated cellulose thin films (SPR-based assay) as well as TOCNF-treated cotton filter paper (Whatman® Grade 4) strips (paper-based assay). Noteworthy, Whatman® filter papers Grades 1 and 4 are often used in this kind of assay due to the best combination of porosity, lateral fluid flow rate, stiffness, and hydrophilicity (Ratajczak & Stobiecka, 2020). TOCNF was produced from softwood kraft pulp according to the protocol described by Saito et al. (Saito et al., 2006) by using a solution of 0.1 mmol/g TEMPO, 1 mmol/g NaBr, and 5 mmol/g NaClO in water at pH 10.5. The reaction was stopped by adding ethanol into the oxidized pulp suspension followed by pH adjustment to 7. Then, the oxidized pulp was washed with deionized water by filtration and diluted to a solids content of 1.5 %. The suspension was dispersed using a high-shear Ystral X50/10 Dispermix mixer for 10 min at 2000 rpm. The resultant suspension was passed twice through a microfluidizer (M110-EH, Microfluidics) at 1800 bar pressure with 400 and 100 μm chambers. The produced TOCNF had 1 mmol/g negatively charged carboxylate groups (conductometric titration). Additionally, TOCNF neutral sugar composition has been analyzed before (Hakalahti et al., 2017). Regenerated cellulose films were prepared from trimethylsilyl cellulose (TMSC) according to Kontturi et al. (Kontturi et al., 2003). Noteworthy, the regenerated cellulose films, as well as cotton filter paper, have low charge densities (Herrington, 2018; Kontturi et al., 2008). Therefore, in this work, the regenerated cellulose thin films are considered as model surfaces for the filter paper in SPR.

2.2. THC detection in surface plasmon resonance (SPR)

2.2.1. Preparation of ultrathin films of TEMPO-oxidized cellulose nanofibrils and regenerated cellulose

TOCNF model films were spin-coated onto PEI-treated gold SPR sensors (Oy BioNavis Ltd., Ylöjärvi, Finland) according to Ahola et al. (Ahola et al., 2008). Briefly, 0.15 wt% TOCNF suspension was ultrasonicated at 25 % amplitude for 2 min and spin-coated (Model WS-400 BZ 6NPP/LITE, Laurell Technologies, PA, USA) on the sensors at 3000 rpm for 90 s. The resultant films were dried at 80 °C for 15 min and stored in desiccators. Regenerated cellulose films were prepared on SPR sensors from trimethylsilyl cellulose (TMSC) according to Kontturi et al. (Kontturi et al., 2003). Briefly, 10 g/L TMSC solution in toluene was spin-coated (Model WS-400 BZ 6NPP/LITE, Laurell Technologies, PA, USA) onto gold SPR sensors (Oy BioNavis Ltd., Ylöjärvi, Finland) at 3000 rpm for 90 s. Desilylation of the TMSC surfaces was done by a hydrochloric acid vapor treatment to gain the regenerated cellulose surfaces (Kontturi et al., 2003). All films were allowed to stabilize in water prior to measurements.

2.2.2. Surface plasmon resonance (SPR)

The preparation of anti-IC biointerfaces on TOCNF model films was monitored with a multi-parametric Surface Plasmon Resonance instrument (MP-SPR Model Navi 210A, Oy BioNavis Ltd., Ylöjärvi, Finland). The refractive indices (RI) of the medium in contact with the surface of the SPR sensor correlate very sensitively with the wavelengths and angles of light at which the surface plasmon resonance effect takes place (Jung et al., 1998). The thickness of the adsorbed layer, d, and the adsorbed amount per unit area Δm, were determined with Eqs. (1) (Jung et al., 1998) and (2) (Campbell & Kim, 2007):

$$d = \frac{l_d}{2}\frac{\Delta angle}{x(n_a - n_0)} \quad (1)$$

$$\Delta m = d\rho \quad (2)$$

where Δangle is the change in the SPR angle, l_d is a characteristic evanescent electromagnetic field decay length, x is a sensitivity factor for the sensor obtained after calibration of the SPR (109.94°/RIU), n_0 is the refractive index of the bulk solution (1.334 RIU), n_a is the refractive index of the adsorbed substance and ρ is the packing density of the adsorbed species. A refractive index and packing density for the proteins were assumed to be 1.57 (Jung et al., 1998) and 1.3 g/cm^3 (Campbell & Kim, 2007), respectively. Each SPR measurement was performed at least in duplicate with a constant flow rate of 10 μL/min at 20 °C.

2.2.3. Non-specific adsorption of anti-IC, anti-THC, and THC onto TOCNF

The non-specific adsorption of anti-IC (30 μg/mL) onto TOCNF and regenerated cellulose was monitored in SPR to gain an understanding of driving forces for interactions at pH 5 (50 mM acetate buffer solution). Anti-IC was allowed to adsorb onto substrate cellulose membrane for 20 min after which the surface was rinsed with buffer to remove loosely bound materials. Similar experiments were conducted with anti-THC (15 μg/mL) and THC (1 μg/mL), and adsorption was followed separately onto TOCNF from 10 mM acetate buffer solution at pH 5. Bovine serum albumin (BSA) was applied as a blocking agent (0.1 mg/mL, 15 min) onto TOCNF before anti-THC (15 μg/mL) adsorption from 10 mM acetate buffer solution at pH 5 to see the effect of the blocker on non-specific binding to the cellulose surface.

2.2.4. Conjugation of anti-IC onto TOCNF films and detection of anti-THC + THC immune complex

Anti-IC was conjugated onto TOCNF model films and monitored in-situ with SPR by EDC/NHS chemistry. First, 0.1 M EDC and 0.4 M NHS solution (in 10 mM acetate buffer, pH 5) was injected for 10 min and followed by rinsing with the buffer. Next, anti-IC (15 μg/mL, 10 mM acetate buffer, pH 5) was introduced on the activated TOCNF surface. After 20 min, the TOCNF surface was rinsed with the respective buffer followed by ethanolamine (0.1 M in MilliQ, pH ~8.5) treatment. The ethanolamine was utilized to remove the unreacted NHS groups from the surface. BSA was applied as a blocking agent (0.1 mg/mL, 15 min) onto the anti-IC conjugated TOCNF. The ability of the immobilized anti-IC to detect anti-THC and THC immune complex was tested by adsorbing

anti-THC (15 μg/mL) and THC (2 and 10 μg/mL) to the surface for 20 min. Rinsing with 10 mM acetate buffer solution at pH 5 followed to remove loosely bound molecules. As a reference, the anti-THC (15 μg/mL) binding onto the anti-IC biointerfaces on TOCNF was tested without the presence of THC (0 μg/mL). The effect of the amount of immobilized anti-IC on the binding of anti-THC Fab (15 μg/mL) and THC (2 and 10 μg/mL) immune complex was also tested by omitting the ethanolamine treatment. Furthermore, the ability of physically adsorbed anti-IC (15 μg/mL) to bind the anti-THC (15 μg/mL) and THC (1 μg/mL) immune complex was also tested by omitting the EDC and NHS activation step and ethanolamine treatment.

2.3. Atomic force microscopy (AFM)

Images of the SPR sensors were acquired before and after protein adsorptions with AFM (MultiMode 8 Scanning Probe Microscope, Bruker AXS Inc.) AFM was used to analyze the effect of conjugation treatments on surface topographical changes upon protein adsorption. Tapping mode in air and silicon cantilevers (NSC15/AIBS, MicroMasch) were used to scan 5 × 5 μm^2 surface areas. Three different spots on each sample were imaged and flattening was used in the image processing.

2.4. THC detection in paper-based assays

2.4.1. Conjugation of anti-THC-HRP

Labeling of detection antibody with horseradish peroxidase (HRP) was done with an HRP conjugation kit (ab102890 HRP Conjugation Kit - Lightning-Link®, Abcam). Briefly, 10 μL Lightning-Link modifier reagent was mixed gently with 100 μL of anti-THC Fab (1 mg/mL in 10 mM phosphate buffer at pH 7.4). Then, the antibody solution was mixed with the 400 μg HRP conjugation mix to prepare an antibody-HRP mixture at a 1:4 ratio. The reaction was left to occur for 3 h at room temperature (20–25 °C). Finally, 10 μL Lightning-Link quencher reagent was added and left to react for 30 min.

2.4.2. THC detection on paper assays

Sensing of THC from aqueous solutions was demonstrated on filter paper substrates (Whatman® Grade 4) by conjugating antibodies on test and control zones of the assay. Conjugation was performed by depositing 1 μL drops of TOCNF (1.3 g/L), EDC/NHS (0.1 M EDC and 0.4 M NHS in 10 mM acetate buffer, pH 5), and anti-IC or anti-mouse IgG (0.5 mg/mL in 10 mM phosphate buffer, pH 7.4) on the sensing areas. 3 wt% BSA and 5 wt% casein hydrolysate solutions were applied on the paper substrates as blocking agents to reduce non-specific interactions. The assays were tested with a THC positive sample (5 μg/mL THC, 2.5 μg/mL anti-THC-HRP, 2 wt% fibrinogen, and 2 wt% casein) and a THC negative sample (2.5 μg/mL anti-THC-HRP, 2 wt% fibrinogen, and 2 wt% casein).

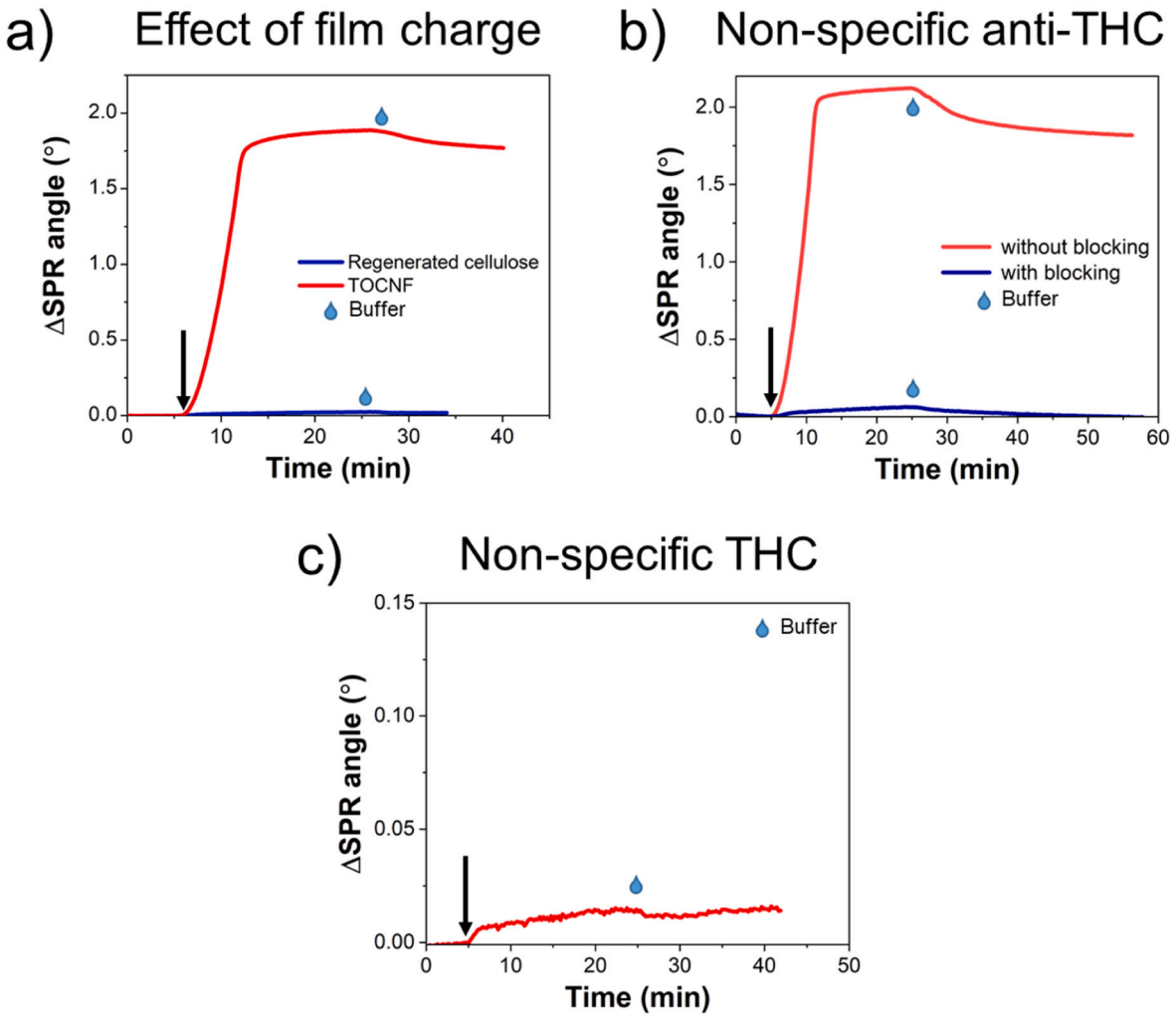

Fig. 1. SPR sensograms: a) 15 μg/mL anti-IC adsorption onto TOCNF and regenerated cellulose at pH 5, b) 15 μg/mL anti-THC adsorption onto TOCNF with (blue) and without (red) BSA blocking at pH 5, and c) 1 μg/mL THC adsorption onto TOCNF at pH 5 (no blocking).

2,2′-azino-bis(3-ethylbenzothiazoline-6-sulfonic acid) (1-Step™ ABTS Substrate Solution, ThermoFisher Scientific) was employed to reach colorimetric results. The analyte samples were deposited from the top.

3. Results and discussion

3.1. Preparation of anti-IC biointerfaces and THC detection in SPR

First, non-specific adsorption of anti-IC Fab onto TOCNF was investigated in SPR at pH 5. Fig. 1a shows the SPR sensogram of the antibody adsorption onto the TOCNF surface, indicating significant attraction of the net positively charged anti-IC (pI 6.5–9.5) (Chiodi et al., 1985) to the negatively charged nanocellulose surface. The adsorbed areal mass of anti-IC was estimated to be as high as 1370 ng/cm^2 (exemplary calculation in SI). The adsorption of the anti-IC was also investigated on a non-charged regenerated cellulose surface, which is considered to model properties of a filter paper, which is later employed as a substrate in paper-based assays. Notably, the regenerated cellulose did not show noteworthy affinity to the antibodies (Fig. 1a and Table 1), revealing that the main driving forces for anti-IC interactions with these cellulose surfaces were indeed electrostatic at pH 5. Next, non-specific interactions between the TOCNF surface, target molecule (THC), and detection antibody (anti-THC) were investigated. Additionally, the effect of BSA on preventing non-specific interactions was studied. Noteworthy, it was revealed that BSA-blocking is a crucial part of the system, and the treatment is needed to ensure specific interactions. Explicitly, Fig. 1b shows high non-specific adsorption of anti-THC (15 μg/mL) onto unmodified TOCNF. Thus, without blocking, this behavior could potentially produce false-positive results or background signals that disturb the THC sensing. To prevent non-specific interactions and to ensure that the detection antibody binds only specifically onto anti-IC in the presence of THC, BSA was added as a blocking agent. The passivation effect of BSA can be seen in Fig. 1b. BSA treatment led to complete passivation of TOCNF surface against non-specific adsorption of anti-THC at pH 5. Furthermore, Fig. 1c shows non-specific adsorption of THC (1 μg/mL) onto TOCNF. The adsorption curve shows that THC alone did not exhibit strong interaction with the TOCNF surface since a low amount was adsorbed onto the surface. The calculated areal masses of the non-specific interactions are collected in Table 1.

SPR was also used to investigate the sensitivity of physically adsorbed anti-IC to THC + anti-THC immune complex on TOCNF surfaces. Interestingly, despite the high amount of adsorbed antibody on TOCNF (Fig. 2a and Table 1), the surface could not bind the immune complex (15 μg/mL anti-THC, 1 μg/mL THC) after blocking treatment with BSA (Fig. 2b and Table 2). Initially, the adsorption of the immune complex was high onto the physically adsorbed anti-IC as a significant positive shift in SPR angle was detected upon injection. However, all immune complexes were removed from the surface upon rinsing, indicating very loose attachment. This behavior suggests that the physically adsorbed anti-IC were attached in non-active conformation preventing proper binding of the target immune complex. Moreover, the immune complex interactions with supramolecular anti-IC biointerface followed a similar trend as compared to the interactions with BSA-blocked TOCNF surface without any antibodies (Fig. 2b). These results were, then, compared with the binding efficiency of chemically conjugated antibodies. To covalently immobilize anti-IC onto the TOCNF surface, EDC/NHS chemistry was utilized. The changes in SPR angle during the antibody conjugation procedure can be seen in Fig. 2c. Notably, after EDC/NHS activation (1), the introduction of anti-IC (2) to the system caused significant adsorption of the antibody onto the activated TOCNF surface. Washing with buffer decreased the SPR angle only slightly. Besides, ethanolamine treatment (pH ~8.5) was used to remove unreacted active sites. Fig. 2c shows a decrease in SPR angle after injection of ethanolamine (3), indicating that the treatment removed loosely bound anti-IC. Most likely the pH change affected the net charge of the proteins, causing changes in electrostatic interactions. This behavior is typical for the system and has been observed previously (Orelma, Filpponen, et al., 2012). Nevertheless, it can be observed that some anti-IC was distinctly covalently immobilized on the TOCNF surface, corresponding to the adsorbed amount of ~187 ng/cm^2 of antibody.

The binding of anti-THC + THC by the immobilized anti-IC on TOCNF was investigated after BSA blocking (BSA adsorption curve can be seen in Fig. S1a). Fig. 2d shows the binding of the immune complex at two THC concentrations (2 and 10 μg/mL) as well as the binding of anti-THC without THC onto the prepared biointerface. As expected, the adsorption of anti-THC without THC (0 μg/mL) onto the TOCNF surface with the immobilized anti-IC was minimal (Table 2). Almost all adsorbed material was rinsed off by the buffer and an areal mass of ~3 ng/cm^2 was obtained. Oppositely, binding of the immune complex was detected upon injection of samples containing both anti-THC and THC. Specifically, the adsorption of the immune complex with 2 μg/mL THC was six times higher compared to the reference, corresponding to the adsorbed amount of ~25 ng/cm^2 after rinsing. Furthermore, when the concentration of THC was increased to 10 μg/mL, the binding of the anti-THC + THC complex was increased to ~35 ng/cm^2. Notably, despite THC being hydrophobic, advantageous interactions occur on the highly hydrated nanocellulose anchor surfaces most likely due to entropy gain upon the expulsion of water molecules. Specifically, it has been shown that water at a protein-ligand interface may have a favorable influence on binding events because the release of thermodynamically unfavorable water molecules, organized at the interfaces, enhance the affinity of ligand during complex formation as well as further binding on the assay biointerface (Ladbury, 1996; Schiebel et al., 2018). Thus, this water-based detection system has the potential for the development of highly sensitive drug assays since aqueous environments can increase the binding affinities of the anti-THC + THC complex.

The effect of ethanolamine treatment on the binding ability of anti-IC was also investigated. By omitting the ethanolamine treatment, a higher amount of anti-IC (~525 ng/cm^2) was attached to the surface since, without the treatment, both loosely adsorbed and covalently attached anti-IC remained on the TOCNF surface (Fig. S1a, b). Nevertheless, the binding of the anti-THC + THC immune complex could not be increased by the higher amount of anti-IC on the surface (Fig. S1c and Table 2). Although a higher concentration of THC (10 μg/mL) resulted in an ~11 % increase in anti-THC + THC immune complex binding without the ethanolamine treatment, the lower concentration of THC (2 μg/mL) lead to a ~ 25 % decrease in the immune complex binding.

Table 1
Anti-IC immobilization and non-specific binding in SPR.

Surface	Conjugate	Adsorbed areal mass (ng/cm^2)
Regenerated cellulose	Anti-IC	11.5 ± 1.27
TOCNF	Anti-IC	1230 ± 198
EDC/NHS activated TOCNF	Anti-IC	525 ± 134
EDC/NHS activated TOCNF	Anti-IC (EA)[a]	187 ± 16.3
TOCNF	Anti-THC	969 ± 228
TOCNF+BSA	Anti-THC	0
TOCNF	THC	7.81 ± 2.26

[a] The areal mass was calculated after removal of loosely bound anti-IC via ethanolamine treatment.

3.2. Topographical changes

AFM imaging was performed to investigate how immobilized antibodies, adsorbed BSA, and the target immune complex altered the surface morphology of the TOCNF films on SPR sensors. The images and height profiles can be seen in Fig. 3. The pristine TOCNF film (Fig. 3a) was uniform and consisted only of nanofibrils (Rq roughness of 1.85 nm). Adsorption of anti-IC on TOCNF (Fig. 3b) produced a film with slightly higher roughness (Rq roughness of 1.98 nm) compared to the pristine film. The supramolecular anti-IC biointerface on TOCNF film after adsorption of BSA and anti-THC + THC immune complex (Fig. 3c)

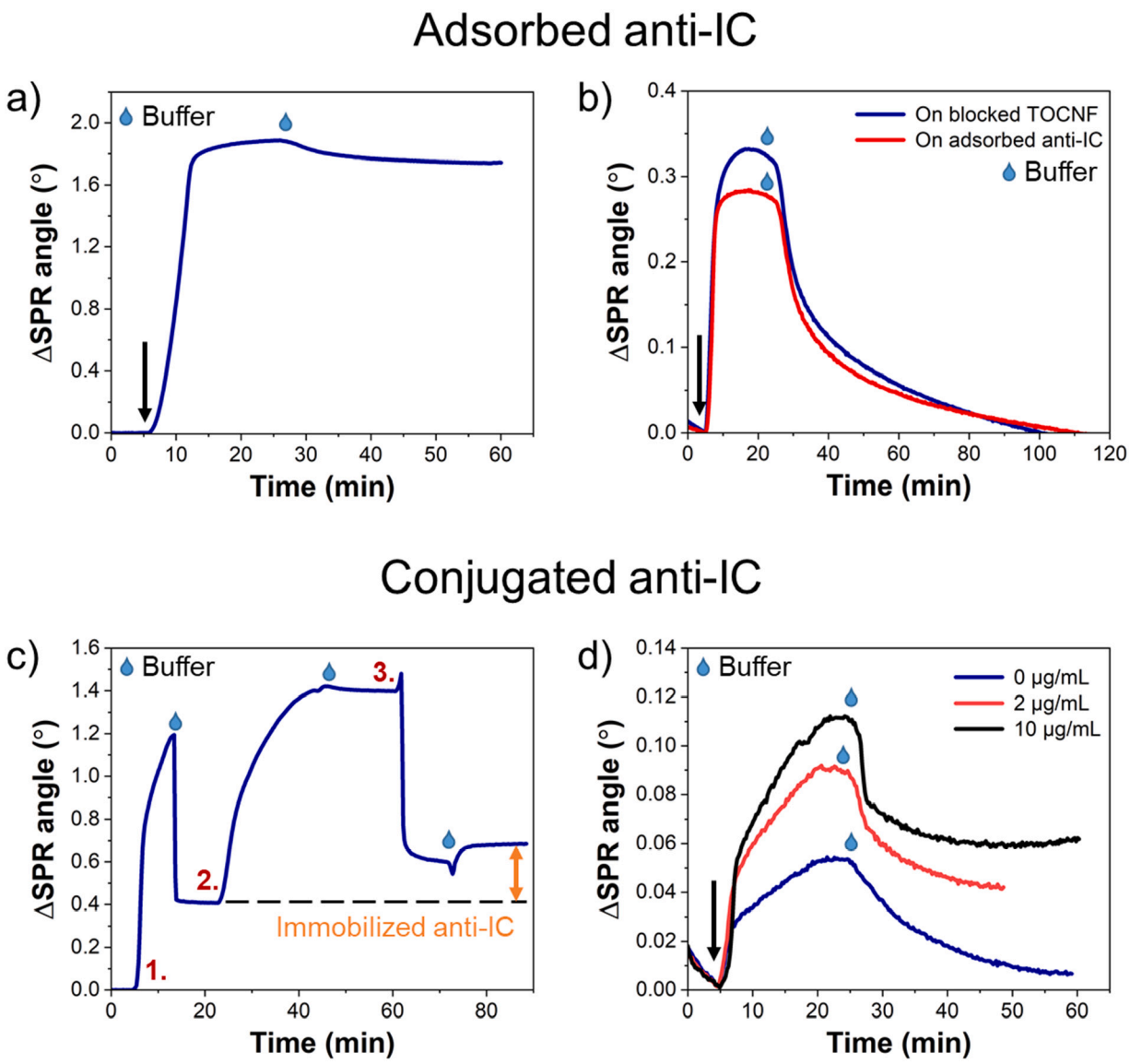

Fig. 2. SPR sensograms: a) Adsorption of anti-IC onto TOCNF. b) Adsorption of anti-THC + THC immune complex with 15 μg/mL anti-THC and 1 μg/mL THC on the physically adsorbed anti-IC surface on TOCNF after BSA treatment (red) and on BSA-blocked TOCNF (blue). c) Conjugation of anti-IC onto TOCNF including (1) EDC/NHS activation followed by (2) anti-IC conjugation and (3) ethanolamine (EA) treatment. d) Adsorption of anti-THC + THC immune complex with 15 μg/mL anti-THC and 2 or 10 μg/mL THC on the conjugated anti-IC surface on TOCNF after BSA treatment, anti-THC (15 μg/mL) binding onto the conjugated anti-IC biointerfaces without the presence of THC (0 μg/mL) is included as a reference.

Table 2
Effect of immobilization method on immune complex (anti-THC + THC) binding on TOCNF surfaces.

Anti-IC immobilization	Anti-THC concentration (μg/mL)	THC concentration (μg/mL)	Adsorbed areal mass (ng/cm^2)[a]
Physical	15	1	0
Conjugation	15	0	3.0 ± 1.61
	15	2	25.5 ± 0.92
	15	10	35.2 ± 3.75
Conjugation +physical (no EA)	15	2	19.1 ± 0.64
	15	10	39.6 ± 3.25

[a] Results obtained from two replicates.

consisted of globular features fully covering the nanocellulose film (Rq roughness of 2.68 nm). Most likely, the globular features are BSA molecules. Similar globular structures can be seen in supramolecular anti-IC biointerface on TOCNF without the immune complex (see Fig. S2a). Moreover, the conjugated anti-IC biointerface on TOCNF film can be seen in Fig. 3d. This film differed significantly from the supramolecular biointerface and consisted of small globular structures, which made the film smoother (Rq roughness of 1.75 nm). After adsorption of BSA and immune complex, the conjugated anti-IC biointerface on TOCNF film (Fig. 3e) showed a structure with bigger fibrillar aggregates (Rq roughness of 3.77 nm). The fibrillar aggregates probably correspond to the adsorbed anti-THC + THC immune complex. Notably, the AFM imaging was performed in the air (dry), and the water removal after adsorptions may have led to protein aggregation.

3.3. Colorimetric detection of THC on the paper assay

EDC/NHS chemistry was utilized to immobilize sensing elements onto the test and control zones of a THC assay on filter paper by using TOCNF as an anchoring layer. In the proposed system, the anti-IC was immobilized on the test zone (T) while a secondary antibody (anti-

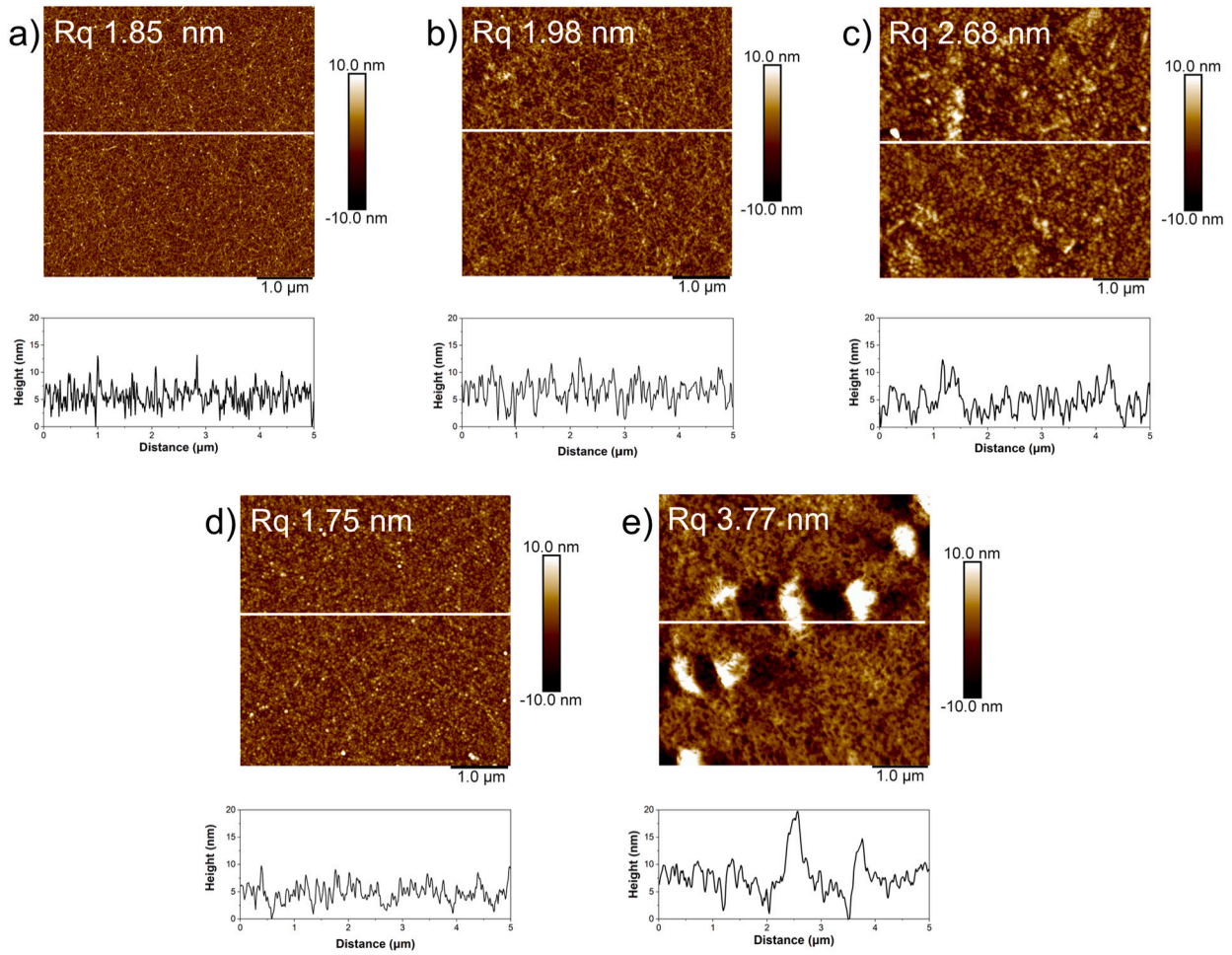

Fig. 3. AFM images and height profiles of samples on SPR sensors: a) pristine TOCNF, b) adsorbed anti-IC biointerface on TOCNF, c) adsorbed anti-IC biointerface on TOCNF after exposure to BSA and THC + anti-THC immune complex, d) conjugated anti-IC biointerface on TOCNF, and e) conjugated anti-IC biointerface on TOCNF after exposure to BSA and immune complex. The height profiles were acquired at the positions indicated with the white lines.

mouse IgG) was attached to the control zone (C). The deposition could be easily done with a pipette. As demonstrated in SPR, the anti-IC binds an immune complex that consists of THC and anti-THC. To detect the binding of the immune complex on paper, anti-THC was labeled with HRP, which can react with 2,2′-azino-bis(3-ethylbenzothiazoline-6-sulfonic acid) (ABTS) to form a green-blue colored product in the presence of hydrogen peroxide. The successful conjugation of the label on the antibody fragment was demonstrated by exposing anti-THC-HRP treated filter paper with ABTS substrate solution (Fig. S3), which produced a vivid green color on the treated area of the paper. Moreover, 3 wt% BSA and 5 wt% casein hydrolysate solutions were applied as blocking agents on the substrate to reduce non-specific adsorption (Fig. S4). The blocking was also done carefully on the sensing areas to ensure that the remaining binding sites on TOCNF were covered with the non-specific proteins.

The assays were tested with THC positive samples (5 µg/mL THC, 2.5 µg/mL anti-THC-HRP, 2 wt% fibrinogen, and 2 wt% casein) and THC negative samples (2.5 µg/mL anti-THC-HRP, 2 wt% fibrinogen, and 2 wt % casein). Fig. 4 shows the schematic illustrations of the binding events on test and control areas with the different samples and the corresponding colorations on the paper assays. Upon testing of the THC negative sample, a green-colored dot appeared only in the control zone (Fig. 4b). Whereas, upon testing of the THC positive sample, colorations occurred on both test and control zones as can be seen in Fig. 4c. The colorimetric results were obtained 10–15 min after applying the solutions. To highlight the importance of the anchor layer and efficient immobilization of antibodies, we performed similar testing on systems without the anchor layer (only antibodies deposited on the substrate) and with only physically immobilized antibodies. Fig. S5 shows that the other systems did not form readable colorations on the sensor substrates, revealing that both the TOCNF anchor layer and chemical conjugation of antibodies are needed to obtain THC detection. Moreover, the suitability of nanocellulose anchor with various printing techniques offers an interesting possibility to develop patterned assays with more precise antibody deposition on a larger scale. Nevertheless, the obtained results indicated quantitative analysis since the intensity of the obtained color results varied between parallel samples. Therefore, as further development of the system, other detection methods such as electrochemical sensing could be tested to offer additional information and insights. In addition, the suitability of nanocellulose anchor with various printing techniques offers an interesting possibility to develop patterned assays with more precise antibody deposition on a larger scale. Additionally, to determine the LOD of the prepared sensor, more experiments based on signal quantification should be performed.

4. Conclusion

Immobilization of antibodies onto TOCNF was demonstrated with EDC/NHS chemistry and employed in THC detection in both SPR and paper assays. The SPR results revealed that EDC/NHS covalent coupling of anti-IC onto TOCNF resulted in robust attachment of the antibody fragment on the surface, confirming our hypothesis. The high surface-to-

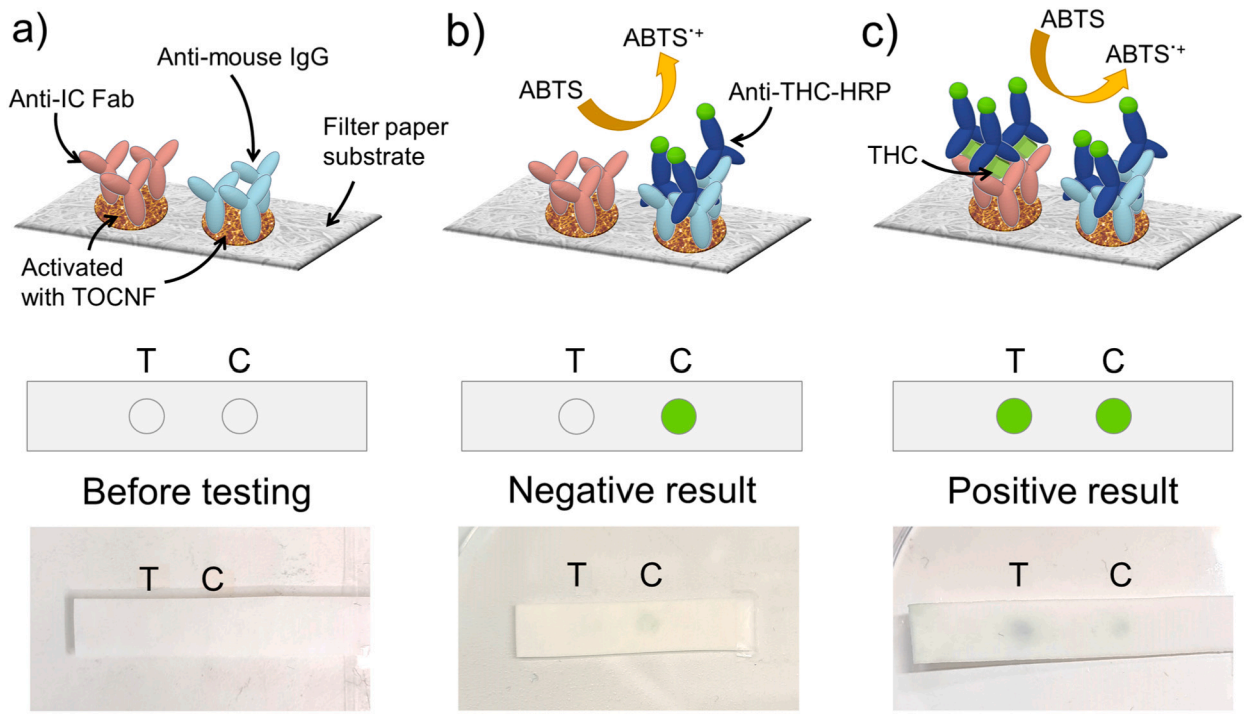

Fig. 4. THC detection on paper assays: a) schematic illustration showing immobilized sensing elements on test and control areas on paper and an image of the untested assay, b) schematic illustration of anti-THC-HRP binding on the control area of the assay without the presence of THC (negative sample) and an image of the colorimetric response with ABTS, c) schematic illustration of immune complex binding on the test area and anti-THC-HRP binding on the control area upon testing with THC-positive sample with an image of the corresponding coloration on paper.

volume ratio, OH-group-rich surface, and high hygroscopicity of TOCNF enabled effective surface functionalization and formation of a hydrophilic spacer for the sensing antibodies. The formed biointerface was able to bind the anti-THC + THC immune complex from an aqueous solution. 1–10 μg/mL THC concentrations were tested, and it was revealed that increasing THC concentration increased the binding of the immune complex by the immobilized anti-IC to some extent. Additionally, the supramolecular adsorption of anti-IC Fab onto TOCNF resulted in a higher antibody amount on surfaces due to attractive charge interactions at pH 5. However, despite that physical adsorption led to a higher anti-IC amount on the surface compared to covalently attached anti-IC, the binding of the immune complex was not supported on the supramolecular biointerface. Most likely, the direct adsorption of the anti-IC on TOCNF reduced its bioactivity or the negative charge of TOCNF disturbed THC adsorption. Further work would be needed to fully understand the complex interfacial phenomena occurring. Additionally, we demonstrated the use of EDC/NHS coupling on paper assays, where the TOCNF anchor was applied and activated on the test and control areas of the assay for antibody immobilization. Colorimetric detection of THC was enabled from aqueous solutions, providing quantitative results. Our approach showed an easy and fast way to control the deposition of THC-sensitive antibodies on surfaces, enabling selective detection of THC from solutions. Here nanocellulose-water interactions were strongly relied upon to form advantageous systems for both the formation of bioactive surfaces and efficient sensing.

CRediT authorship contribution statement

Katariina Solin and Maija Vuoriluoto contributed equally to this paper.

Alexey Khakalo and Tekla Tammelin are Corresponding authors.

Declaration of competing interest

The authors declare that they have no known competing financial interests or personal relationships that could have appeared to influence the work reported in this paper.

Data availability

No data was used for the research described in the article.

Acknowledgments

This project was funded by the European Union's Horizon 2020 research and innovation programme under grant agreement No 760876. This work was part of the Academy of Finland Flagship Programme under projects No. 318890 and 318891 (Competence Center for Materials Bioeconomy, FinnCERES). Katariina Solin and Maija Vuoriluoto contributed equally. The manuscript was written through the contributions of all authors. All authors have approved the final version of the manuscript.

Appendix A. Supplementary data

Supplementary data to this article can be found online at https://doi.org/10.1016/j.carbpol.2022.120517.

References

Aguilar-Sanchez, A., Jalvo, B., Mautner, A., Nameer, S., Pöhler, T., Tammelin, T., & Mathew, A. P. (2021). Waterborne nanocellulose coatings for improving the antifouling and antibacterial properties of polyethersulfone membranes. *Journal of Membrane Science, 620*, Article 118842. https://doi.org/10.1016/J.MEMSCI.2020.118842

Aguilar-Sanchez, A., Jalvo, B., Mautner, A., Rissanen, V., Kontturi, K. S., Abdelhamid, H. N., Tammelin, T., & Mathew, A. P. (2021). Charged ultrafiltration membranes based on TEMPO-oxidized cellulose nanofibrils/poly(vinyl alcohol)

antifouling coating. *RSC Advances, 11*(12), 6859–6868. https://doi.org/10.1039/D0RA10220B

Ahola, S., Salmi, J., Johansson, L. S., Laine, J., & Österberg, M. (2008). Model films from native cellulose nanofibrils. Preparation, swelling, and surface interactions. *Biomacromolecules, 9*(4), 1273–1282. https://doi.org/10.1021/bm701317k

Alkhamis, O., Canoura, J., Bukhryakov, K. V., Tarifa, A., DeCaprio, A. P., & Xiao, Y. (2021). DNA aptamer–cyanine complexes as generic colorimetric small-molecule sensors. *Angewandte Chemie International Edition*. https://doi.org/10.1002/ANIE.202112305

Arola, S., Tammelin, T., Setälä, H., Tullila, A., & Linder, M. B. (2012). Immobilization-stabilization of proteins on nanofibrillated cellulose derivatives and their bioactive film formation. *Biomacromolecules, 13*(3), 594–603. https://doi.org/10.1021/bm201676q

Berthet, A., de Cesare, M., Favrat, B., Sporkert, F., Augsburger, M., Thomas, A., & Giroud, C. (2016). A systematic review of passive exposure to cannabis. *Forensic Science International, 269*, 97–112. https://doi.org/10.1016/J.FORSCIINT.2016.11.017

Campbell, C. T., & Kim, G. (2007). SPR microscopy and its applications to high-throughput analyses of biomolecular binding events and their kinetics. *Biomaterials, 28*(15), 2380–2392. https://doi.org/10.1016/j.biomaterials.2007.01.047

Chiodi, F., Sidén, Å., & Ösby, E. (1985). Isoelectric focusing of monoclonal immunoglobulin G, A and M followed by detection with the avidin-biotin system. *Electrophoresis, 6*(3), 124–128. https://doi.org/10.1002/ELPS.1150060305

Hakalahti, M., Faustini, M., Boissière, C., Kontturi, E., & Tammelin, T. (2017). Interfacial mechanisms of water vapor sorption into cellulose nanofibril films as revealed by quantitative models. *Biomacromolecules, 18*(9), 2951–2958. https://doi.org/10.1021/acs.biomac.7b00890

Heise, K., Kontturi, E., Allahverdiyeva, Y., Tammelin, T., Linder, M. B., Nonappa, & Ikkala, O. (2021). Nanocellulose: recent fundamental advances and emerging biological and biomimicking applications. *Advanced Materials, 33*, Article 2004349. https://doi.org/10.1002/adma.202004349

Helander, A., Johansson, M., Andersson, A., & Villén, T. (2021). Analytical and medico-legal problems linked to the presence of delta-8-tetrahydrocannabinol (delta-8-THC): Results from urine drug testing in Sweden. *Drug Testing and Analysis*. https://doi.org/10.1002/DTA.3190

Herrington, T. M. (2018). The surface potential of cellulose. In *Papermaking raw materials, Trans. of* (pp. 165–181). https://doi.org/10.15376/frc.1985.1.165

Huestis, M. A., Mitchell, J. M., & Cone, E. J. (1996). Urinary excretion profiles of 11-Nor-9-carboxy-Δ9-tetrahydrocannabinol in humans after single smoked doses of marijuana. *Journal of Analytical Toxicology, 20*(6), 441–452. https://doi.org/10.1093/JAT/20.6.441

Jung, L. S., Campbell, C. T., Chinowsky, T. M., Mar, M. N., & Yee, S. S. (1998). Quantitative interpretation of the response of surface plasmon resonance sensors to adsorbed films. *Langmuir, 14*(19), 5636–5648. https://doi.org/10.1021/la971228b

Kale, N. (2019). Urine drug tests: Ordering and interpreting results. *American Family Physician, 99*(1), 33–39. www.aafp.org/afp.

Kidwell, D. A., Holland, J. C., & Athanaselis, S. (1998). Testing for drugs of abuse in saliva and sweat. *Journal of Chromatography B: Biomedical Sciences and Applications, 713*(1), 111–135. https://doi.org/10.1016/S0378-4347(97)00572-0

Kontturi, E., Thüne, P. C., & Niemantsverdriet, J. W. (2003). Cellulose model surfaces-simplified preparation by spin coating and characterization by X-ray photoelectron spectroscopy, infrared spectroscopy, and atomic force microscopy. *Langmuir, 19*(14), 5735–5741. https://doi.org/10.1021/la0340394

Kontturi, K. S., Tammelin, T., Johansson, L. S., & Stenius, P. (2008). Adsorption of cationic starch on cellulose studied by QCM-D. *Langmuir, 24*(9), 4743–4749. https://doi.org/10.1021/la703604j

Ladbury, J. E. (1996). Just add water! The effect of water on the specificity of protein-ligand binding sites and its potential application to drug design. *Chemistry and Biology, 3*(12), 973–980. https://doi.org/10.1016/S1074-5521(96)90164-7

Lam, T., Devadhasan, J. P., Howse, R., & Kim, J. (2017). A chemically patterned microfluidic paper-based analytical device (C-μPAD) for point-of-care diagnostics. *Scientific Reports, 7*(1). https://doi.org/10.1038/s41598-017-01343-w

Lee, J. R., Choi, J., Shultz, T. O., & Wang, S. X. (2016). Small molecule detection in saliva facilitates portable tests of marijuana abuse. *Analytical Chemistry, 88*(15), 7457–7461. https://doi.org/10.1021/acs.analchem.6b01688

Leppänen, I., Lappalainen, T., Lohtander, T., Jonkergouw, C., Arola, S., & Tammelin, T. (2022). Capturing colloidal nano- and microplastics with plant-based nanocellulose networks. *Nature Communications, 13*(1), 1–12. https://doi.org/10.1038/s41467-022-29446-7, 2022 13:1.

Li, Y., Uddayasankar, U., He, B., Wang, P., & Qin, L. (2017). Fast, sensitive, and quantitative point-of-care platform for the assessment of drugs of abuse in urine, serum, and whole blood. *Analytical Chemistry, 89*(16), 8273–8281. https://doi.org/10.1021/acs.analchem.7b01288

Mahmoudifard, M., Soudi, S., Soleimani, M., Hosseinzadeh, S., Esmaeili, E., & Vossoughi, M. (2016). Efficient protein immobilization on polyethersolfone electrospun nanofibrous membrane via covalent binding for biosensing applications. *Materials Science and Engineering: C, 58*, 586–594. https://doi.org/10.1016/J.MSEC.2015.09.007

Niemi, M. H., Turunen, L., Pulli, T., Nevanen, T. K., Höyhtyä, M., Söderlund, H., Rouvinen, J., & Takkinen, K. (2010). A structural insight into the molecular recognition of a (-)-δ9-tetrahydrocannabinol and the development of a sensitive, one-step, homogeneous immunocomplex-based assay for its detection. *Journal of Molecular Biology, 400*(4), 803–814. https://doi.org/10.1016/j.jmb.2010.05.048

O'Farrell, B. (2009). Evolution in lateral flow-based immunoassay systems. In *Lateral Flow Immunoassay* (pp. 1–33). Humana Press. https://doi.org/10.1007/978-1-59745-240-3_1.

Orelma, H., Filpponen, I., Johansson, L. S., Österberg, M., Rojas, O. J., & Laine, J. (2012). Surface functionalized nanofibrillar cellulose (NFC) film as a platform for immunoassays and diagnostics. *Biointerphases, 7*(1–4), 1–12. https://doi.org/10.1007/s13758-012-0061-7

Orelma, H., Johansson, L. S., Filpponen, I., Rojas, O. J., & Laine, J. (2012). Generic method for attaching biomolecules via avidin-biotin complexes immobilized on films of regenerated and nanofibrillar cellulose. *Biomacromolecules, 13*(9), 2802–2810. https://doi.org/10.1021/bm300781k

Orelma, H., Morales, L. O., Johansson, L. S., Hoeger, I. C., Filpponen, I., Castro, C., Rojas, O. J., & Laine, J. (2014). Affibody conjugation onto bacterial cellulose tubes and bioseparation of human serum albumin. *RSC Advances, 4*(93), 51440–51450. https://doi.org/10.1039/c4ra08882d

Orelma, H., Teerinen, T., Johansson, L. S., Holappa, S., & Laine, J. (2012). CMC-modified cellulose biointerface for antibody conjugation. *Biomacromolecules, 13*(4), 1051–1058. https://doi.org/10.1021/bm201771m

Pelton, R. (2009). Bioactive paper provides a low-cost platform for diagnostics. *TrAC - Trends in Analytical Chemistry, 28*(8), 925–942. https://doi.org/10.1016/j.trac.2009.05.005

Plouffe, B. D., & Murthy, S. K. (2017). Fluorescence-based lateral flow assays for rapid oral fluid roadside detection of cannabis use. *Electrophoresis, 38*(3–4), 501–506. https://doi.org/10.1002/elps.201600075

Raghav, R., & Srivastava, S. (2016). Immobilization strategy for enhancing sensitivity of immunosensors: L-Asparagine–AuNPs as a promising alternative of EDC–NHS activated citrate–AuNPs for antibody immobilization. *Biosensors and Bioelectronics, 78*, 396–403. https://doi.org/10.1016/J.BIOS.2015.11.066

Ratajczak, K., Sklodowska-Jaros, K., Kalwarczyk, E., Michalski, J. A., Jakiela, S., & Stobiecka, M. (2022). Effective optical image assessment of cellulose paper immunostrips for blood typing. *International Journal of Molecular Sciences, 23*(15), 8694. https://doi.org/10.3390/ijms23158694

Ratajczak, K., & Stobiecka, M. (2020). High-performance modified cellulose paper-based biosensors for medical diagnostics and early cancer screening: A concise review. In , *229*. *Carbohydrate Polymers* (p. 115463). Elsevier. https://doi.org/10.1016/j.carbpol.2019.115463.

Saito, T., Nishiyama, Y., Putaux, J. L., Vignon, M., & Isogai, A. (2006). Homogeneous suspensions of individualized microfibrils from TEMPO-catalyzed oxidation of native cellulose. *Biomacromolecules, 7*(6), 1687–1691. https://doi.org/10.1021/bm060154s

Schiebel, J., Gaspari, R., Wulsdorf, T., Ngo, K., Sohn, C., Schrader, T. E., Cavalli, A., Ostermann, A., Heine, A., & Klebe, G. (2018). Intriguing role of water in protein-ligand binding studied by neutron crystallography on trypsin complexes. *Nature Communications, 9*(1), 1–15. https://doi.org/10.1038/s41467-018-05769-2

Shmanai, V. V., Nikolayeva, T. A., Vinokurova, L. G., & Litoshka, A. A. (2001). Oriented antibody immobilization to polystyrene macrocarriers for immunoassay modified with hydrazide derivatives of poly(meth)acrylic acid. *BMC Biotechnology, 1*(1), 1–5. https://doi.org/10.1186/1472-6750-1-4

Solin, K., Beaumont, M., Rosenfeldt, S., Orelma, H., Borghei, M., Bacher, M., Opietnik, M., & Rojas, O. J. (2020). Self-assembly of soft cellulose nanospheres into colloidal gel layers with enhanced protein adsorption capability for next-generation immunoassays. *Small, 2004702*. https://doi.org/10.1002/smll.202004702

Solin, K., Orelma, H., Borghei, M., Vuoriluoto, M., Koivunen, R., & Rojas, O. J. (2019). Two-dimensional antifouling fluidic channels on nanopapers for biosensing. *Biomacromolecules, 20*(2), 1036–1044. https://doi.org/10.1021/acs.biomac.8b01656

Stanković, V., Đurđić, S., Ognjanović, M., Antić, B., Kalcher, K., Mutić, J., & Stanković, D. M. (2020). Anti-human albumin monoclonal antibody immobilized on EDC-NHS functionalized carboxylic graphene/AuNPs composite as promising electrochemical HSA immunosensor. *Journal of Electroanalytical Chemistry, 860*, Article 113928. https://doi.org/10.1016/J.JELECHEM.2020.113928

Stevenson, H., Bacon, A., Joseph, K. M., Gwandaru, W. R. W., Bhide, A., Sankhala, D., Dhamu, V. N., & Prasad, S. (2019). A rapid response electrochemical biosensor for detecting Thc in saliva. *Scientific Reports, 9*(1), 1–11. https://doi.org/10.1038/s41598-019-49185-y, 2019 9:1.

Takkinen, K., Söderlund, H., & Pulli, T. (2011). *Detection of cannabis use (US20110086364A1)*.

Thapa, D., Samadi, N., Patel, N., & Tabatabaei, N. (2020). Enhancement of sensitivity and detection limit of lateral flow immunoassays using lock-in thermography. *Biophotonivs in Point-of-Care, 11361*(13), 24. https://doi.org/10.1117/12.2555274

United Nations Office on Drugs and Crime. (2021). Drug market trends: Cannabis opioids. In *World Drug report*. www.unodc.org/unodc/en/data-and-analysis/wdr2021.html.

Vuoriluoto, M., Orelma, H., Lundahl, M., Borghei, M., & Rojas, O. J. (2017). Filaments with affinity binding and wet strength can be achieved by spinning bifunctional cellulose nanofibrils. *Biomacromolecules, 18*(6), 1803–1813. https://doi.org/10.1021/acs.biomac.7b00256

Yetisen, A. K., Akram, M. S., & Lowe, C. R. (2013a). Paper-based microfluidic point-of-care diagnostic devices. *Lab on a Chip, 13*(12), 2210–2251. https://doi.org/10.1039/c3lc50169h

Yetisen, A. K., Akram, M. S., & Lowe, C. R. (2013). Paper-based microfluidic point-of-care diagnostic devices. In , *13*. *Lab on a chip* (pp. 2210–2251). Royal Society of Chemistry. https://doi.org/10.1039/c3lc50169h. Issue 12.

Zuurman, L., Ippel, A. E., Moin, E., & van Gerven, J. M. A. (2009). Biomarkers for the effects of cannabis and THC in healthy volunteers. *British Journal of Clinical Pharmacology, 67*(1), 5–21. https://doi.org/10.1111/J.1365-2125.2008.03329.X